Journal of
Synchrotron
Radiation

ISSN 0909-0495

Received 13 March 2009
Accepted 8 July 2009

An attempt to analyze the bark disease in *Havea brasiliensis* using X-ray absorption near-edge spectroscopy

Wanwisa Pattanasiriwisawa,[a]* Nualpun Sirinupong,[a,b] Pluang Suwanmanee,[c] Chatchamon Daengkanit[d] and Jaruwan Siritapetawee[e]

[a]Synchrotron Light Research Institute, 111 University Avenue, Muang, Nakhon Ratchasima 30000, Thailand, [b]Biochemistry and Molecular Biology, Wayne State University, School of Medicine, 540 E. Canfield Avenue, Detroit, MI 48201, USA, [c]Biology Department, Faculty of Science, Thaksin University, Songkhala 90000, Thailand, [d]Surat Thani Rubber Research Center, Tha Chana District, Surat Thani 84170, Thailand, and [e]Ubonratchathani University, College of Medicine and Public Health, Ubon Rajathanee University, Ubon Ratchathani 34190, Thailand.
E-mail: wanwisa@slri.or.th

The X-ray absorption near-edge spectroscopy (XANES) technique has been used to determine the chemical change of elements induced by bark diseases in *Havea brasiliensis* (rubber latex tree). The results show the good sensitivity of *in situ* XANES for characterizing the chemical structure of phosphorus, sulfur, potassium and calcium in healthy and diseased *Havea brasiliensis*. Important information for understanding the bark disease involved in the sulfur metabolism of plants was also obtained from XANES.

Keywords: XANES; rubber; *Hevea brasiliensis*; tapping panel dryness; bark necrosis.

1. Introduction

Hevea brasiliensis (rubber latex tree), a perennial tropical tree originating in South America, is mostly cultivated in Southeast Asia for the production of natural rubber. The unique isoprenoid compound *cis*-1,4-polyisoprene present in latex is the raw material for the world's rubber. Natural rubber is highly valued because no synthetic substitute has comparable elasticity, resilience and resistance to high temperature. Natural rubber is mainly used by the tyre industry and is still essential for automotive components. Rubber is also used for military purposes and utilized in a variety of other products.

A rubber tree is subject to many types of diseases that must be controlled for economic production. There are two kinds of bark diseases known to limit rubber yield: tapping panel dryness (TPD) and trunk phloem necrosis (TPN) or bark necrosis (BN). However, the causes of both diseases are unknown. TPD is favoured by various factors (Gohet & Keli, 1994) and has been reported to be linked to sugar depletion (Lacrotte *et al.*, 1997) and/or oxidative stress in the latex cells and inner bark (Das *et al.*, 1998). Most often, TPD extends from the tapping cut downwards to the bottom part of the trunk. Some genes are involved in the protection against deleterious effects induced by oxidative stress (Kongsawadworakul, 1997). This disease becomes more serious with the increasing age of the plantation and can be induced by yield stimulation with ethylene (Chrestin, 1989). TPD has a strong association with ethylene, with the potential of this gaseous plant hormone to cause much physiological damage to the cells including programmed cell death in TPD-affected tissues (Krishnakumar *et al.*, 2001). TPN or BN, diagnosed in 1984, is an irreversible bark disease of complex origin, with inner soft bark tissue necrosis (Nandris *et al.*, 1991). TPN generally starts from the rootstock–scion junction (all trees in a plantation are grafted clones), spreading upward along the trunk above the tapping cut. TPN disease involves impairment of the cyanogenic metabolism in the rubber tree trunk. The cDNAs of enzymes involved in cyanide metabolism (linamarase, hydroxynitrile lyase and cyanoalanine synthase) have been cloned from the *Hevea sp.* phloem specific cDNA library (Nandris *et al.*, 2004).

TPN is favoured by adverse environment conditions, such as soil and climate (especially in marginal areas such as in the east, northeast and the north of Thailand), by anthropogenetical stresses (methods of planting and exploitation), and probably by some physiological rootstock–scion incompatibility (Pellegrin *et al.*, 2004). At the early stage of these bark diseases, it is impossible to visually discriminate between TPD and TPN, and therefore it is impossible to give the adapted recommendations to the planters in time. These bark diseases become more and more important in plantations, and often seriously affect the rubber yield, as most of the plants are no longer tapped. In the absence of a definitive cause, there exists a general consensus in the literature that TPD and TPN are a metabolic disorder or molecular physiological syndrome. It is therefore necessary to set up molecular

physiological tools to analyze the chemistry and internal structure of wood in parallel with biochemical and molecular diagnostic tools, and to select or even create new rubber clones exhibiting low sensitivity to these diseases. However, all these characteristics [the rubber yield potential (latex flow and regeneration) and the sensitivity to these bark disease] are known to depend on rubber clones (Chrestin, 1989) and therefore on cell chemistry and the internal structure of wood.

The motivation for our studies is based on the fact that Thailand is the largest rubber exporter in the world. The X-ray absorption near-edge spectroscopy (XANES) technique is useful for identifying chemical forms (as fingerprints) and oxidation states as well as studying valence states (Prange *et al.*, 2002). Therefore this is a good opportunity for us to analyze the nutrients in bark disease (*e.g.* P, S, K and Ca) using XANES because these mineral nutrients are important to the plant's life cycle. The nutrients are divided into three main categories: macroelements, microelements and beneficial elements. All mineral nutrients are necessary for a healthy nutrient-rich plant. Macroelements, *e.g.* carbon, hydrogen and oxygen, make up the backbone of all biomolecules, and are supplied by the air and water. Six other macroelements are found in soils: nitrogen is required by plants to make amino acids, proteins, enzymes and the light-capturing molecule chlorophyll; phosphorus is the backbone of DNA reproductive and RNA coding for making biomolecules, and is required for energy transfer; potassium is required for moving sugars and carbohydrates within plants, and for plant adjustments to drought conditions; calcium is required for plant cell walls (Demarty *et al.*, 1984; Kinzel, 1989) and root growth; sulfur is required for plant synthesis of sulfur-containing amino acids and metabolism (Jalilehvand, 2006; Prange *et al.*, 2005).

The information gained from this study may point the way to identifying the origin and the activating mechanisms of TPD and TPN in *Hevea brasiliensis*, leading to a molecular physiological tool for early diagnosis of these major bark diseases in the field to be used as recommendations to the planters. The optimal exploitation system would be adapted to certain rubber clones under given environmental conditions. Moreover, basic knowledge of other diseases in *Hevea brasiliensis* would also be provided. Subsequently, the production of rubber trees with resistance to stress or disease, and pathogens for bark diseases would be accomplished.

2. Experiment

2.1. Sample preparation

Leaves and bark fragments were collected from *Hevea* clone BPM24 which has provided high rubber yields but not disease endurance (Suwanmanee *et al.*, 2007). There were three samples each of leaves and bark: healthy rubber trees (used as controls), TPD and BN. Samples intended for analysis by X-ray fluorescence were dried and ground until they were well blended. The samples intended for analysis by XANES were sliced into small (about 2 mm square) pieces, but not ground, so as to preserve the cell structure. These cell-preserved leaf samples were temperature controlled for analysis by XANES. Fresh leaves and bark from healthy and diseased trees were used for RNA extraction and cDNA-AFLP analysis.

2.2. X-ray fluorescence

Elemental analysis of the sample powders was carried out at the X-ray fluorescence (XRF) laboratory of the Natural Metal and Materials Technology Center (MTEC), Thailand. The dried ground bark and leaves were polished with deionized water to assure surface homogeneity and then the element compositions were determined in duplicate by XRF using a Philips PW-2404 spectrometer equipped with a Cr tube.

2.3. cDNA amplified fragments length polymorphism (cDNA-AFLP)

For all leaves and bark samples, the total RNA was extracted by following Suwanmanee *et al.* (2002) and Asif *et al.* (2000). The integrity of the RNA was examined on a denaturing agarose gel. Poly(A)$^+$ RNA was prepared from total RNA with an Oligotex mRNA kit (Qiagen Inc., Valencia, CA, USA) as described by the manufacturer's instructions. Finally, double-stranded cDNA was synthesized from poly(A)$^+$ RNA using the cDNA synthesis system (Promega, Mandison, WI, USA) according to the kit protocol. The cDNA-AFLP procedure described by Bachem *et al.* (1996, 1998) was utilized with minor modifications. The cDNA was completely digested with EcoRI and PstI endonuclease and then ligated to EcoRI and PstI double-strand adapters. The ligation was used as a template for the pre-amplified DNA fragments with the corresponding pre-amplification primers without extension. The pre-amplified products were diluted 20-fold and used for selective amplification. A total of ten primer combinations having two selective nucleotides at the 3′ end (EcoRI+2/PstI+2 combination) were used for the selective amplification. The products were separated on a 6% polyacrylamide gel containing urea and TBE according to Sambrook *et al.* (1989). The cDNA bands were stained with silver nitrate, according to Bassam *et al.* (1991).

2.4. XANES measurements

All cell-preserved leaf samples were stuck to a rectangular frame of size 12 mm × 10 mm. The *in situ* XANES experiment was performed at the XAS station beamline 8 (BL8) of the Synchrotron Light Research Institute (SLRI, Thailand). The flux at the sample is around 10^8–10^{10} photon s^{-1} (100 mA)$^{-1}$ and the energy resolution ($\Delta E/E$) is around 10^{-4} (Klysubun *et al.*, 2007). A Si(111) double-crystal monochromator was used to monochromate X-ray beams for the *K*-edge measurement of sulfur, potassium and calcium, and an InSb(111) crystal for the *K*-edge measurements of phosphorus in fluorescence mode. The XANES spectrum was recorded using two ionization chambers which were placed before and on the left-hand side of the sample. The first ionization chamber, placed before the sample, was filled with 40 mbar air for the phosphorus, 60 mbar air for the sulfur, 400 mbar of N_2 gas for the

Table 1
Element compositions as determined using XRF in leaves and bark of healthy, TPD and BN *Hevea* trees.

N/D = not determined.

	Concentration (wt%)					
	Control healthy leaves	TPD leaves	BN leaves	Control healthy barks	TPD barks	BN barks
O	27.09	26.4	28.76	26.74	26.54	26.66
Na	0.19	0.23	0.24	<0.01	N/D	<0.01
Mg	6.32	5.94	7.89	1.15	2.07	3.04
Al	0.04	0.04	0.14	0.04	0.03	N/D
Si	0.84	0.74	1.84	0.04	0.5	0.38
P	5.9	5.36	5.45	0.53	0.71	0.95
S	2.01	2.38	1.08	0.51	0.34	0.23
K	26.96	19.47	14.19	5.2	5.02	3.73
Ca	13.5	16.81	23.53	57.88	54.8	54.32
Mn	0.46	0.54	0.47	0.57	0.52	0.43
Fe	0.21	0.21	0.2	<0.01	<0.01	<0.01
Ni	<0.01	<0.01	<0.01	<0.01	<0.01	<0.01
Cu	0.04	<0.01	<0.01	<0.01	<0.01	<0.01
Rb	0.14	0.11	0.11	<0.01	<0.01	<0.01
Sr	0.05	0.06	0.05	0.18	0.14	0.13
W	<0.01	<0.01	N/D	<0.01	<0.01	N/D
Total	83.75	78.29	83.95	92.8	90.7	89.9

calcium *K*-edge and 250 mbar air for the potassium *K*-edge measurements. A polypropylene window is used to separate the sample chamber from the first ionization chamber. The second ionization chamber is a Lytle detector or five-grid ionization detector which was placed on the left-hand side of the sample. The sample chamber flows with He gas. The exposure time is around 8–10 min per sample. All of the XANES spectra were averaged and normalized using *IFEFFIT* software (version 1.2.11) (Ravel & Newville, 2005).

3. Results and discussion

3.1. XRF analysis

Table 1 shows the element composition of leaves and bark from healthy and bark-diseased (TPD and BN) rubber trees as determined using XRF. The leaves and bark of rubber trees are mainly composed of the elements oxygen, potassium, calcium, magnesium, phosphorus and sulfur; these mineral nutrients are necessary for a healthy and nutrient-rich plant. Oxygen makes up the backbone of all biomolecules and is supplied by the air and water. Five other macroelements are found in soils which were uptaken by the plants through the root xylem–phloem system. Other detectable elements are microelements and beneficial elements, which are equally important to the plant's life cycle, although required in lesser amounts. There are some minerals which are detected in significantly different amounts in healthy and diseased rubber trees. Magnesium and silicon are detected in higher amounts in diseased bark and in BN leaves than in healthy trees. In the same way, phosphorus and calcium are shown in higher amounts in the diseased bark and leaves, whereas the amount of phosphorous and potassium in diseased leaves is lower than in healthy leaves. In addition, sulfur is lower in diseased bark as in BN leaves. Consequently, the elements which are detectable in the diseased bark are in lesser amounts than in healthy bark.

3.2. cDNA-AFLP analysis

The total RNA isolated from the leaves and bark of *Hevea* clone BPM24 gave an OD_{260}/OD_{280} ratio (where OD is the optical density) of 1.94 $\pm$ 0.2 and 1.98 $\pm$ 0.5, respectively, indicating that the total RNA was of high purity and appeared to be intact from electrophoresis in 1% agarose gel. There were sharp and clear separations of the 28S rRNA and 18S rRNA bands. The gene expression profiles of healthy and diseased tree were visualized by separating the amplified cDNA on 6% polyacrylamide gel and stained with silver nitrate. The gene expression profiles of healthy trees and disease in leaves and bark are shown in Figs. 1 and 2, respectively. The total transcript-derived fragments (TDFs) in the leaves and bark show different expression patterns for each combination primer between healthy and diseased plants. Among ten combinations primers there are several differentially TDFs as shown by arrows in Figs. 1 and 2. For example, in leaves, Fig. 1 primers 4 and 6, there are TDFs above and less than 500 base pairs (bp), respectively, presented only in the control healthy tree, but not in TPD and BN. In the same way, in bark, Fig. 2 primers 5 and 6, there are TDFs about 400 bp and 700 bp, respectively, presented only in the healthy tree. These cDNA fragments are interesting because they are expressed only in the control healthy tree and not in the diseased tree. Ten combinations of AFLP primers produced 454 TDFs in leaves and a total of 438 TDFs were found in bark as shown in detail in Table 2. This observation indicates that these differently expressed genes are involved in TPD and BN, as well as the different shape of the sulfur *K*-edge XANES spectrum in healthy and diseased trees.

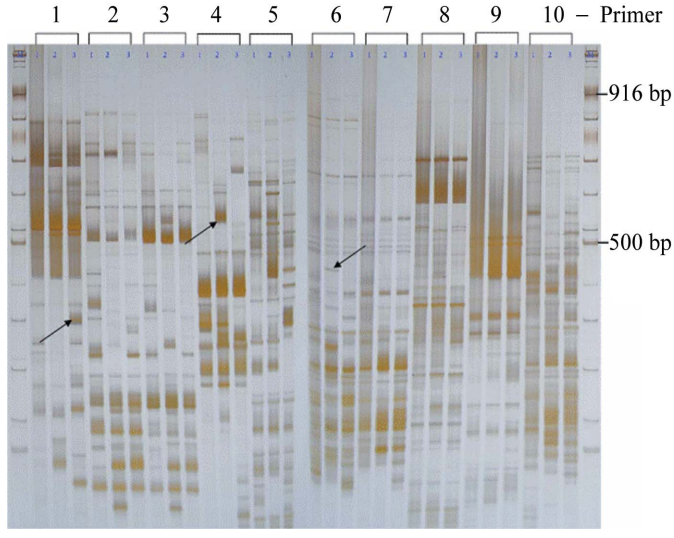

Figure 1
Gene expression profile in leaves for TPD, control healthy and BN, shown in lanes 1, 2 and 3, respectively. The arrows point to examples of differentially amplified cDNA fragments among each primer 1, 4 and 6.

Table 2
Transcript-derived fragments, produced by ten combinations of AFLP primers in leaves and bark of healthy, TPD and BN *Hevea* trees.

	Transcript-derived fragments					
	Leaves			Barks		
	Control healthy	TPD	BN	Control healthy	TPD	BN
1	11	10	14	14	10	11
2	13	20	16	17	14	10
3	12	12	12	14	15	12
4	12	13	11	8	14	7
5	20	22	22	9	4	12
6	19	20	21	24	25	25
7	12	19	17	22	20	21
8	18	16	14	19	16	17
9	6	6	9	7	10	10
10	15	20	22	14	15	22
	138	158	158	148	143	147
Total	454			438		

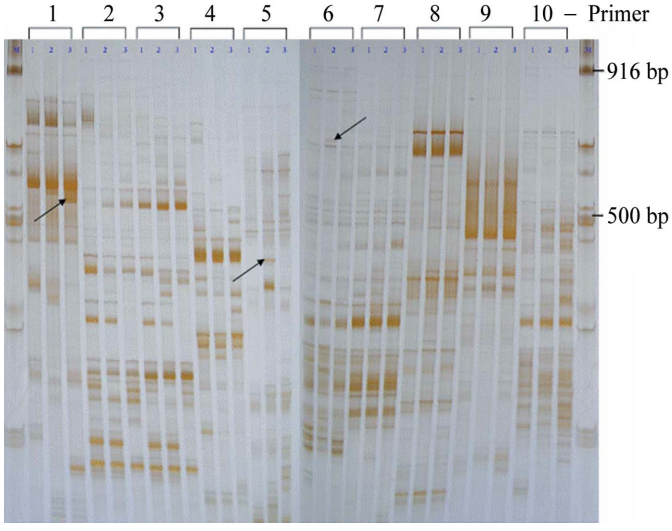

Figure 2
Gene expression profile in barks for TPD, control healthy and BN, shown in lanes 1, 2 and 3, respectively. The arrows point to examples of differentially amplified cDNA fragments among each primer 1, 5 and 6.

3.3. XANES analysis

The XANES spectra, shown in Figs. 3–6, are used for the identification of minerals (phosphorus, sulfur, potassium and calcium) in the healthy and bark-diseased leaves. Fifty-four leaves were investigated for each element. However, we used only cell-preserved leaf samples because the disease affects the organism or metabolism. The metabolism of diseased plants can be investigated using leaf samples (Prange *et al.*, 2005; Jalilehvand, 2006). The result of this metabolism should be the same either in leaves or bark. It is also easy to collect samples and perform this experiment. Fig. 3 shows the *K*-edge XANES of phosphorus in the control normal, TPD and BN which match with the reference compound (ferric phosphate dihydrate; $FePO_4{\cdot}2H_2O$). The standard ferric phosphate dihydrate also coincides with the phosphorus *K*-edge located at 2152 eV (Fig. 3). The result exhibits the highly specific element pattern of XANES when the neighbouring atoms of

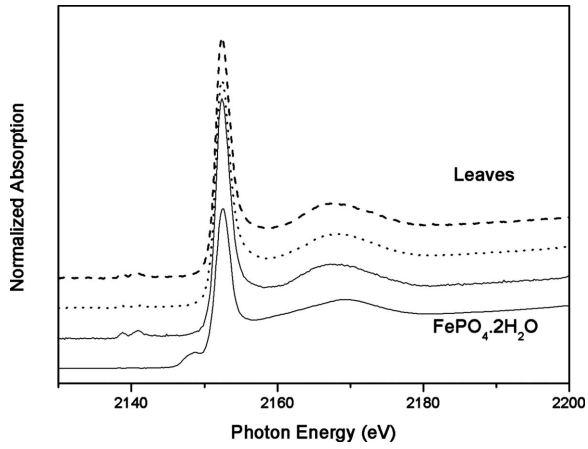

Figure 3
Phosphorus *K*-edge spectra of leaves: normal control healthy (solid line), TPD (dashed line) and BN disease (dotted line).

the absorbent atom are different. There is a small peak at 2148.23 eV of the *K*-edge XANES spectrum of phosphorus contained within $FePO_4{\cdot}2H_2O$ (solid line) in contrast with the struvite ($NH_4MgPO_4{\cdot}4H_2O$) spectrum. All of the *K*-edge XANES spectra are the same, which means that bark disease does not have any detectable effect on the average local environment of the macronutrient phosphorus, either through metabolic disorder or molecular physiological syndrome.

Sulfur is an important element for metabolism (Jalilehvand, 2006; Prange *et al.*, 2005). The primary sulfate (SO_4^{2-}) is the most oxidative sulfur present in soil and uptakes sulfur into the root of the plant. Plants assimilate primary sulfate which is subsequently subjected to activation to adenosine 5′-phosphosulfate (5′-adenylylsulfate [APS]) for further conversion. APS is reduced to sulfite (SO_3^{2-}) and sulfide (S^{2-}) in the major assimilatory pathway (Saito, 2004). The major chemical forms of sulfur in leaves are thiol (—SH) and thioether groups, disulfides, sulfoxides, sulfonate ($R—SO_3^-$) and sulfates (Jalilehvand, 2006). The XANES spectrum of the *K*-edge of sulfur of the control healthy leaves, TPD, BN and standard references [L-cystine, L-methionine, cysteic acid ($C_3H_7NO_5S$) and zinc sulfate] are shown in Fig. 4. The standard zinc sulfate ($ZnSO_4$) also coincides with the sulfur *K*-edge located at 2481.4 eV (Fig. 4). XANES measurement of the *K*-edge of sulfur shows a maximum at the location of the first peak where electrons are excited to the valence state (white line) for standard zinc sulfate ($ZnSO_4$). The sulfur *K*-edge XANES spectrum feature showed similar sulfur species with peaks at 2472.30, 2475.04, 2479.93 and 2481.13 eV. These peaks can be assigned to the thiol, σ^* (S—O), $R—SO_3$ and $R—SO_4$. The assignment of the peaks is based on the studies of Hitchcock *et al.* (1986), Sze *et al.* (1988), George & Gorbaty (1989), Prange *et al.* (2005) and Jalilehvand (2006). Our result shows that there is some difference between the sulfonate and sulfates peaks of the sulfur *K*-edge XANES spectrum in healthy and diseased samples. The σ^* peak of S—O (2475 eV) is also decreased. It might be that the sulfur is oxidizing with oxygen, and the sulfur has changed chemically from $R—SO_3$ to $R—$

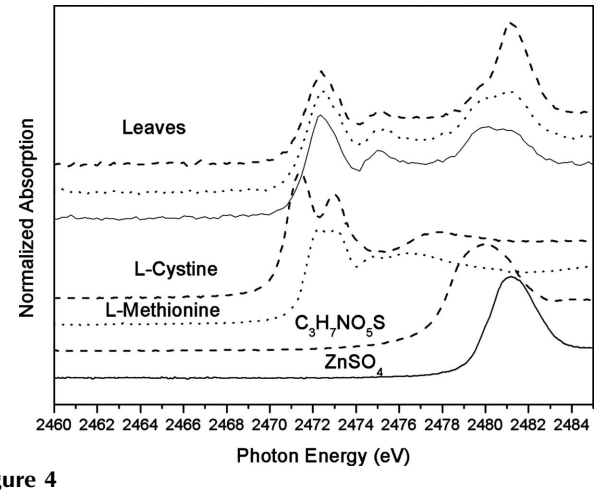

Figure 4
Sulfur *K*-edge spectra of leaves: normal control healthy (solid line), TPD (dashed line) and BN disease (dotted line).

SO_4. It seems that bark disease has an effect on the metabolism of sulfur.

Potassium is an important nutrient for plant growth and reproduction (*i.e.* photosynthesis, control of ionic balance and activation of plant enzymes). The XANES spectrum of the *K*-edge of potassium of control healthy leaves, TPD, BN and standard references [potassium iodide (KI) and potassium chloride (KCl)] are shown in Fig. 5. Our result shows that the shape of the XANES spectrum has the same characteristics as in healthy or diseased rubber trees. This implies that the disease does not significantly affect the coordination around most of the potassium within the cells of the plants. Also, the spectrum is not similar to the reference compounds (KI and KCl). In the future, the characterization of potassium in the plants should be found.

Finally, the calcium structures in the leaves of a plant were investigated by measuring the *K*-edge on XANES spectra. The maximum of the first peak of calcium oxalate monohydrate ($CaC_2O_4{\cdot}H_2O$, whewellite) is located at 4052.09 eV (Fig. 6). The XANES spectra of the calcium *K*-edge of the control healthy leaves, TPD, BN and standard reference

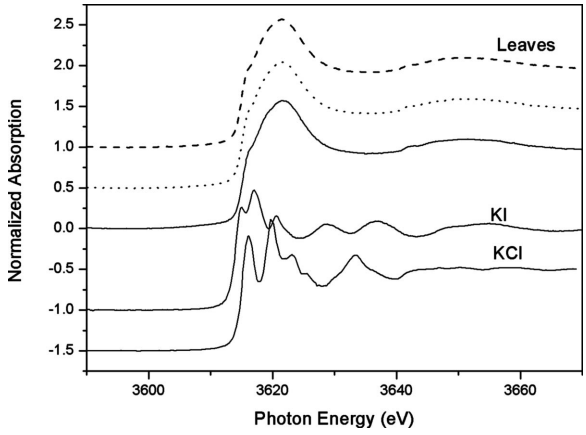

Figure 5
Potassium *K*-edge spectra of leaves: control healthy (solid line), TPD (dashed line) and BN disease (dotted line).

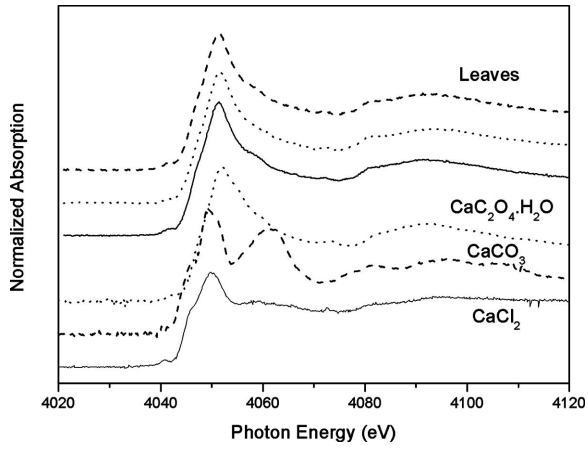

Figure 6
Calcium *K*-edge spectra of leaves: control healthy (solid line), TPD (dashed line) and BN disease (dotted line).

compounds [calcium carbonate ($CaCO_3$), calcium chloride ($CaCl_2$) and calcium oxalate ($CaC_2O_4{\cdot}H_2O$)] are shown in Fig. 6. Calcium is involved in many mechanisms such as stabilization of the cell wall (Kinzel, 1989; Demarty *et al.*, 1984), ion exchange properties (Demarty *et al.*, 1984) and developed pathways (Bush, 1995). Calcium forms calcium oxalate in many organs or tissues in plants such as roots, stems, leaves, flowers, fruits and seed (Franceschi & Horner, 1980), and epidermal (Zindler-Frank, 1975) and vascular tissue (Wang *et al.*, 1994). Our results show that the shape of an XANES spectrum is similar to that of calcium oxalate either in healthy or diseased rubber trees. This means that the disease has no obvious effect on the average speciation of calcium within the plant cell.

Radiation damage can occur due to many factors such as the photon energy, dose and exposure time (Ascone *et al.*, 2003; Pickering & George, 2007). In our experiment the radiation damage of samples was also a concern. We scanned two different areas in each sample and observed the XANES spectrum. The XANES spectra were quite reproducible. All of the samples were also visually inspected for variations in colour, shape and morphology of cells. In all of the samples the same features still remained as prior to entering the experiment. This indicates that the radiation damage on the leaf samples was negligible during the XAS measurements.

4. Conclusion

In situ XANES spectra of healthy and diseased (TPD and BN) rubber trees show different shapes at the sulfur *K*-edge which is significant for plant synthesis and metabolism. This information will help us to understand how bark diseases occur in *Hevea brasiliensis*. XANES is a useful non-destructive method for analyzing chemical structures.

XRF analysis showed that minerals are required for the proper functioning of plant life in several ways: controlling the growth in metabolic pathways, defending and developing cell functions, and reproduction. The nutritious elements must be in the correct forms and amounts for them to be taken up into

the system and benefit the plant. Therefore, minerals improve the overall quality and health of plants in which nutrients are deficient (or excessive) and may have caused nutrient imbalance leading to disease being observed in the healthy and TPD or BN rubber trees.

The cDNA-AFLP analysis was useful for identifying differently expressed genes between healthy and TPD or BN *Hevea* trees. The candidate genes with regard to TPD or BN are to be further cloned and characterized. Their role and function could provide potential insight into the biological or metabolic processes in TPD and BN.

This research is supported by the Synchrotron Light Research Institute.

References

Ascone, I., Meyer-Klaucke, W. & Murphy, L. (2003). *J. Synchrotron Rad.* **10**, 16–22.

Asif, M. H., Dhawan, P. & Nath, P. (2000). *Plant Mol. Biol. Rep.* **18**, 109–115.

Bachem, C. W. B., Oomen, R. J. F. J. & Visser, R. G. F. (1998). *Mol. Biol. Rep.* **16**, 157–173.

Bachem, C. W. B., Van Der Hoeven, R. S., De Bruijn, S. M., Vreugdenhil, D., Zabeau, M. & Visser, R. G. F. (1996). *Plant J.* **9**, 745–753.

Bassam, B. J., Anollés, G. C. & Gresshoff, P. M. (1991). *Anal. Biochem.* **196**, 80–83.

Bush, D. S. (1995). *Annu. Rev. Plant Physiol. Plant Mol. Biol.* **46**, 95–122.

Chrestin, H. (1989). *Physiology of Rubber Tree Latex*, edited by J. d'Auzac, J. L. Jacob and H. Chrestin, pp. 431–441. Boca Raton: CRC Press.

Das, G., Raj, S., Pothen, J., Sethuraj, M. R., Sinha, T. P. & Sen-Mandi, S. (1998). *Plant Physiol. Biochem.* **25**, 47–50.

Demarty, M., Morvan, C. & Thellier, M. (1984). *Plant Cell Environ.* **7**, 441–448.

George, G. N. & Gorbaty, M. L. (1989). *J. Am. Chem. Soc.* **111**, 3182–3186.

Gohet, E. & Tran Van Canh Keli, J. (1994). *Proceedings of the IRRDB Workshop on Tapping Panel Dryness of Hevea*, Hainan, China, pp. 37–49.

Franceschi, V. R. & Horner, H. T. (1980). *Bot. Rev.* **46**, 361–427.

Hitchcock, A. P., Horsley, J. A. & Stöhr, J. (1986). *J. Chem. Phys.* **85**, 4835–4848.

Jalilehvand, F. (2006). *Chem. Soc. Rev.* **35**, 1256–1268.

Kinzel, H. (1989). *Flora*, **182**, 99–125.

Klysubun, W., Sombunchoo, P., Wongprachanukul, N., Tarawarakarn, P., Klinkhico, S., Chaiprapa, J. & Songsiriritthigul, P. (2007). *Nucl. Instrum. Methods Phys. Res. A*, **582**, 87–89.

Kongsawadworakul, P. (1997). MSc Thesis, Mahidol University, Thailand, p. 213.

Krishnakumar, R., Annamalainathan, K. & Jacob, J. (2001). *Ind. J. Nat. Rubber Res.* **14**, 14–19.

Lacrotte, R., Vichitcholchai, N., Cherstin, H., Pujade-Renaud, V., Kosaisave, J., Sri-Sarn, P., Narangajavana, J., Montoro, P. & Gidrol, X. (1997). *Proceeding of the Seminar on the Biochemical and Molecular Tools for Exploitation Diagnostic and Rubber Tree Improvement*, Thailand, p. LX-1–27.

Nandris, D., Chrestin, H., Noirot, M., Nicole, M., Thouvenel, J. C., Rio, B. & Geiger, J. P. (1991). *Eur. J. For. Pathol.* **21**, 325–339.

Nandris, D., Moreau, R., Pellegrin, F., Chrestin, H., Abina, J. & Angui, P. (2004). *Plant Dis.* **88**, 1047.

Pellegrin, F., Nandris, H., Chrestin, H. & Duran-Vila, N. (2004). *Plant Dis.* **88**, 1046.

Pickering, I. J. & George, G. N. (2007). *AIP Conf. Proc.* **882**, 311–315.

Prange, A., Chauvistré, R., Modrow, H., Hormes, J., Trüper, H. G. & Dahl, C. (2002). *Microbiology*, **148**, 267–276.

Prange, A., Oerke, E. C., Steiner, U., Bianchetti, C. M., Hormes, J. & Modrow, H. (2005). *J. Phytopathol.* **153**, 627–632.

Ravel, B. & Newville, M. (2005). *J. Synchrotron Rad.* **12**, 537–541.

Saito, K. (2004). *Plant Physiol.* **136**, 2443–2450.

Sambrook, J., Fritsch, E. F. & Maniatis, T. (1989). *Molecular Cloning – A Laboratory Manual*, 2nd ed. New York: Cold Spring Harbour Laboratory Press.

Suwanmanee, P., Sirinupong, N., Dangsawang, P., Dangkanit, C., Chocknukul, S. & Nuntanuwat, W. (2007). *STT 33 Congress on Science and Technology of Thailand*, Thailand, Abstracts, p. 256.

Suwanmanee, P., Suvachittanon, W. & Fincher, G. B. (2002). *Sci. Asia*, **28**, 29–36.

Sze, K. H., Brion, C. E., Tronc, M., Bodeur, S. & Hitchcock, A. P. (1988). *Chem. Phys.* **121**, 279–297.

Wang, Z. Y., Gould, K. S. & Patterson, K. J. (1994). *Int. J. Plant Sci.* **155**, 342–349.

Zindler-Frank, E. (1975). *Z. Pflanzenphysiol.* **77**, 80–85.